


2 **Geochemistry and sediment in the main stream of the Ca River**
3 **basin, Vietnam: weathering process, solute-discharge**
4 **relationships, and reservoir impact**

5 **Ho Thi Phuong**¹  · **Kenji Okubo**² · **Md. Azhar Uddin**²

6 Received: 24 November 2018 / Revised: 6 February 2019 / Accepted: 26 February 2019
7 © Science Press and Institute of Geochemistry, CAS and Springer-Verlag GmbH Germany, part of Springer Nature 2019

8 **Abstract** In this study, we investigated the chemical
9 composition of dissolved solids in the Ca River basin,
10 North-Central Vietnam. Water samples were collected
11 from August 2017 to July 2018 at three hydrological sta-
12 tions located in the main stream of the Ca River. Carbonate
13 weathering was found as the dominant process controlling
14 the water chemistry in that area. The average concentra-
15 tions of dissolved solids generally decreased from upstream
16 to downstream, resulting in low concentrations of the major
17 ions in the downstream basin. Variations in the concen-
18 trations of major chemical ions and suspended solids at
19 discharge were also investigated. Major chemical weath-
20 ering products were found to behave chemostatically with
21 increasing discharges upstream. However, dilution behav-
22 iors of solutes were shown in both midstream and down-
23 stream. Primary evidence shows that water storage in
24 reservoirs impacts a variety of suspended solids and dis-
25  solved solids in the Ca River.

27 **Keywords** Ca River · Dissolved solids · Geochemistry ·
28 Carbonate weathering · Suspended solids

1 Introduction

The natural chemical compositions and transport fluxes in
rivers depend on multiple environmental factors such as
sources (lithosphere, atmosphere, biosphere), sinks (vege-
tation uptake, settling), rate-controlling factors (tempera-
ture, water circulation), and drainage basin area (Meybeck
1994; Milliman and Farnsworth 2011). Atmospheric pol-
lution and human activity can have significant effects on
the natural geochemistry of river basins (Chetelat et al.
2008; Li et al. 2009; Li and Zhang 2008; Roy et al. 1999).
Detailed geochemical studies have quantified major ion
compositions (Li and Zhang 2008; Maharana et al. 2015),
weathering processes (Chetelat et al. 2008; Sarin et al.
1989), long-term fluxes (Negrel et al. 2007; Sarin et al.
1989), and controlling factors in solute exports from vari-
ous scales of basins (Godsey et al. 2009; Musolff et al.
2015). Some have researched natural river geochemistry,
where basins with minimal human activity—such as hilly
headwater basins (Bruijnzeel 1983) and unpolluted or less-
polluted river basins (Meybeck 1994)—were considered.
However, establishing natural background values is chal-
lenging because most major rivers are already polluted or
exposed to long-range transport of atmospheric pollutants
(Meybeck and Helmer 1989).

Rivers in Vietnam, like many other rivers around the
world, have been impacted by economic development.
Reservoirs of various sizes have been constructed along the
rivers for power generation, water supply, and flood control
(Amos et al. 2017). In addition, other anthropogenic
activities (e.g., intensive agriculture, land-use change, and
industrial development) can have significant impacts on
how natural river materials move. However, geochemical
data for Vietnamese rivers are sparse. Thus, we investi-
gated the geochemistry of the Ca River, one of the large

A1  Ho Thi Phuong
A2 phuongmt.dhv@gmail.com

A3 ¹ School of Chemical, Biological and Environmental
A4 Technologies, Vinh University, 182, Le Duan Street,
A5 Vinh City, Nghe an, Vietnam

A6 ² Graduate School Environmental and Life Science, Okayama
A7 University, 3-1-1, Tsushima-Naka, Kita-ku,
A8 Okayama 700-8530, Japan

63 basins in north-central Vietnam, covering an area of
 64 27,200 km². Major ion chemistries were determined at
 65 sites upstream of the reservoirs, which were primarily
 66 under forest cover, and at sites mid- and downstream,
 67 below the reservoirs. Weathering processes controlling the
 68 major geochemistry were also determined. Additionally,
 69 variations in the concentrations of major chemical ions and
 70 suspended solids in the discharge were investigated.

71 2 Study area

72 The Ca River is an international river located between
 73 18°15'00"N to 20°10'30"N and 103°45'20"E to
 74 105°15'20"E (Fig. 1). The basin covers 27,200 km²,
 75 including 17,730 km² in Vietnam's territory and 9470 km²
 76 in Laos. The main river originates from Mt. Muong Khut
 77 and Muong Lap (1800–2000 m) in Laos, flows from
 78 northwest to southeast, enters into the Nghe An, Thanh
 79 Hoa, and Ha Tinh provinces of Vietnam, and flows out to
 80 the Eastern Sea at the Hoi estuary. Total river length is
 81 531 km, of which 170 km runs through Laos and 361 km
 82 is in Vietnam. Forests in the Ca River basin are largely
 83 located upstream of three Laos provinces (Bolikhamsay,
 84 Xieng Khouang, and Houaphanh). In Vietnam, forests are
 85 concentrated north, northwest, and southwest of the basin
 86 at elevations of 150–1500 m (IWRP 2012). The catchment
 87 is covered primarily by forest (44%) and agricultural crops
 88 (18%) (Chikamori et al. 2012). Area soils are formed from
 89 parent rocks, Ferralsol in particular (83.51%) (IWRP 2012;
 90 Nauditt and Ribbe 2017). Other soil types are Fluvisol and
 91 Acrisol. The Ca River basin is located in a monsoon cli-
 92 mate, and rainfall is distributed over the year, which has
 93 two distinct seasons: the dry season and the rainy season. In
 94 the upper reaches of the river, the rainy season is from May
 95 to October, but downstream, it is from June to November.

Average annual precipitation in the basin is
 1100–2500 mm.

Multiple reservoirs have been constructed in the Ca
 River basin, namely Ban Ve, Khe Bo, Thac Muoi, and Sao
 reservoirs. These multi-purpose reservoirs are used for
 hydropower generation, water supply, irrigation, and flood
 and drought control. Ban Ve is the largest among them and
 is located at approximately 100 m elevation. Its gross
 capacity is 1835×10^6 m³, and its effective capacity is
 1383×10^6 m³.

Samples were obtained from the main stream of the Ca
 River at My Ly (104°18'54"E and 19°36'51"N), Dua
 (105°02'20"E and 18°59'20"N), and Yen Thuong
 (105°23'00"E and 18°41'10"N). My Ly is located
 approximately 215 m above the Ban Ve reservoir (70 km).
 It covers 1190 km² or 4.4% of the total drainage basin.
 Located in the high mountains and covered primarily by
 forest, the My Ly basin is sparsely populated and is subject
 to little human impact. Both Dua and Yen Thuong are
 downstream of all reservoirs, covering 20,800 km² and
 23,000 km² (76.5% and 84.6% of the river basin),
 respectively. Both are strongly influenced by human
 activity (e.g., agriculture and mining activities). Addition-
 ally, water storage and reservoir operations impact the Ca
 River and its resources.

3 Sampling and analytical methods

From August 2017 to July 2018, 121 water samples were
 collected from three hydrological stations in the main
 stream of the Ca River basin. During the flood season,
 water samples were collected four to six times monthly,
 and during the dry season, they were collected one to four
 times monthly. Samples were representative of the range of
 discharge rates.

Each sample of 2 L, collected from an average depth of
 10 cm at the river bank, was placed in high-density poly-
 ethylene containers then immediately cooled and main-
 tained at a low temperature until analysis. Concentrations
 of the major cations (Ca²⁺, Mg²⁺, Na⁺, and K⁺), anions
 (HCO₃⁻, SO₄²⁻, Cl⁻, NO₃⁻, and PO₄³⁻), and dissolved silica
 (SiO₂) were determined in the laboratory. Cation and most
 anion concentrations were found using ion chromatography
 (Shimadzu, Japan). Dissolved silica and phosphate were
 measured using a DR900 (HACH) colorimeter. Water
 samples were filtered through pre-washed 0.45-μm Milli-
 pore membrane filters before ion concentrations were
 determined. Additionally, the concentration of suspended
 solids was determined by filtering 100 mL sample through
 a 0.45-μm membrane filter (Whatman). Finally, the total

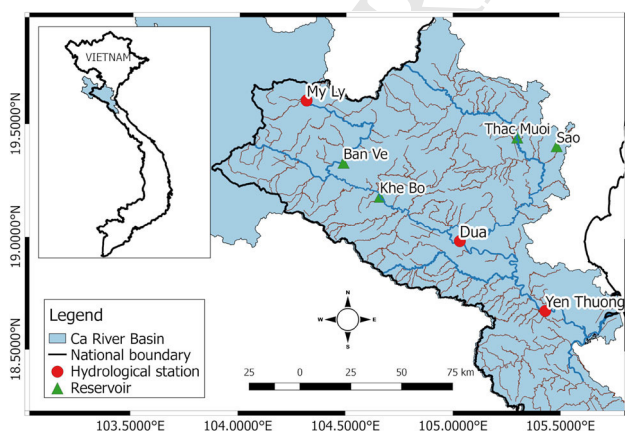


Fig. 1 Map of the Ca River basin

144 concentration of all dissolved solids was the sum of the
145 major elements plus dissolved silica.

146 4 Results and discussion

147 4.1 Contributions of chemical compositions

148 The concentration of each major chemical in the main
149 stream of the Ca River basin is given in Table 1. Total
150 dissolved solids (TDS) varied from 77 to 205 mg/L,
151 averaging 144 mg/L, higher than the world average,
152 100 mg/L (Milliman and Farnsworth 2011). The average
153 value for TDS is comparable to that reported for the Hong
154 (176 mg/L) in Vietnam, but it is lower than that reported
155 for the Son in India (227 mg/L) and the Upper Han River
156 in China (248 mg/L) (Li and Zhang 2008; Maharana et al.
157 2015; Moon et al. 2007). Compared with the rivers drain-
158 ing in areas dominated by silicate rock, such as the upper
159 Ganjiang (63 mg/L) and rivers in the Southeast Coastal
160 Region of China (75.2 mg/L), TDS in the Ca River is much
161 higher (Liu et al. 2018; Ji and Jiang 2012). However, it is
162 much lower compared to the Huanghe (557 mg/L) and
163 Tarim (1000 mg/L), both of which drain in areas domi-
164 nated by evaporite dissolution (Fan et al. 2014; Xiao et al.
165 2012). Bedrock lithology plays a critical role in controlling
166 the character and quantity of the total delivered (Meybeck
167 1987; Milliman and Farnsworth 2011). Human activity also
168 significantly influences TDS values [e.g., in the Liao River
169 of China (400 mg/L) and several European rivers (Ding
170 et al. 2016; Milliman and Farnsworth 2011)].

171 The total cationic charge ($Tz^+ = 2Ca^{2+} + 2Mg^{2+} + K^+$
172 $+Na^+$) ranged from 1145–2981 $\mu eq/L$, averaging 2119
173 $\mu eq/L$. The total anionic charge ($Tz^- = HCO_3^- + 2SO_4^{2-} +$
174 $Cl^- + NO_3^- + 3PO_4^{3-}$) ranged from 811 to 2271 $\mu eq/L$,
175 averaging 1567 $\mu eq/L$. The extent of $Tz^+ - Tz^-$ charge
176 imbalance, characterized by the normalized inorganic
177 charge balance [$NICB = (Tz^+ - Tz^-)/Tz^+$], is related to
178 the contributions of other anions (Li et al. 2009; Ji and
179 Jiang 2012).

180 Calcium was the dominant cation, ranging in concen-
181 tration from 381 to 1005 μM , accounting for an average of
182 62.0% of the total cation charge. Magnesium followed,
183 ranging from 102 to 368 μM , accounting for an average of
184 23.2% of the total cation charge, then sodium (12.3%) and
185 potassium (2.4%) followed. Bicarbonate was the dominant
186 anion, ranging from 600 to 2039 μM , accounting for 84.4%
187 of the total anion charge. Chloride and sulfate together
188 comprised 12.6% of the total anion charge in nearly equal
189 proportions. Nitrate and phosphate contributed negligible
190 proportions (2.7 and 0.3%, respectively).

Dissolved Si ranged in concentration from 133 to 191
250 μM , averaging 202 μM , comprising an average of 192
8.6% of the TDS. It ranked third in abundance after HCO_3^- 193
(55.8%) and Ca^{2+} (18.3%). Compared to other major ions, 194
dissolved Si was relatively independent of lithology, 195
remaining constant between 80 and 160 $\mu mol/L$ SiO_2 (ex- 196
cept in streams draining volcanic rocks, where it reaches 197
350 $\mu mol/L$ SiO_2) (Meybeck 1987). Dissolved Si content 198
is, however, controlled by the climate (temperature and 199
rainfall) (White and Blum 1995). 200

4.2 Spatial and seasonal variations of major solutes and suspended solids

203 The total concentrations of major solutes at My Ly ranged 203
from 142 to 205 mg/L, averaging 168 mg/L. At Dua, TDS 204
varied from 85 to 171 mg/L, averaging 138 mg/L. On the 205
other hand, the TDS value at Yen Thuong ranged from 77 206
to 167 mg/L, averaging 128 mg/L. Generally, the total 207
solute concentration decreased from upstream to down- 208
stream, consistent with decreased concentrations of the 209
major ions Ca^{2+} , Mg^{2+} , Na^+ , Cl^- , HCO_3^- , SO_4^{2-} , and SiO_2 210
in the downstream basin. The observed spatial variations in 211
solute concentrations in the main stream of the Ca River 212
could be related to the effects of tributary inflows, resulting 213
in dilution. A downstream trend in K^+ concentration was 214
not significant, reflecting its conservative behavior in the 215
basin. An increase in NO_3^- concentration in the down- 216
stream basin might have been from anthropogenic sources 217
such as agricultural activity and untreated sewage (Maha- 218
rana et al. 2015). 219

220 The study period was divided into two sub-periods: the 220
wet season (June to November for Dua and Yen Thuong 221
and May to October for My Ly) and the dry season (De- 222
cember to May and November to April, respectively) 223
(Fig. 2). Trends in seasonal solute variations were similar 224
between Dua and Yen Thuong. The concentrations of 225
almost all tested ions increased from the wet to dry sea- 226
sons, indicating the dilution effect of greater atmospheric 227
precipitation during the rainy season. For that reason, at 228
Dua and Yen Thuong, the total solute concentration 229
increased from the wet to dry seasons. At My Ly, however, 230
TDS decreased slightly from the wet to dry seasons, a 231
result of decreased concentration in the major ion HCO_3^- . 232
Other elements remained constant when comparing the two 233
seasons. Phosphate concentration increased in the wet 234
season at all stations, indicating the contribution of organic 235
matter degradation (at My Ly) or human activity (at Dua 236
and Yen Thuong). 237

238 Normally, suspended sediment concentration (SSC) 238
decreases from upstream to downstream and from the wet 239
to dry seasons (Fig. 2). In our case, it greatly varied from 240

Table 1 Chemical compositions of the rivers in the Ca River basin

Stations	Date	Discharge m ³ /s	Na ⁺ mg/l	K ⁺ mg/l	Ca ²⁺ mg/l	Mg ²⁺ mg/l	Cl ⁻ mg/l	SO ₄ ²⁻ mg/l	HCO ₃ ⁻ mg/l	NO ₃ ⁻ mg/l	PO ₄ ³⁻ mg/l	SiO ₂ mg/l	NIBC	TSS mg/l
My Ly	13/08/2017	172	4.65	1.30	30.43	7.89	1.15	4.28	120.80	–	0.13	12	0.12	54
	20/08/2017	154	13.87	1.73	18.74	6.68	7.93	6.00	97.60	–	0.16	13	0.08	41
	27/08/2017	198	14.20	2.76	24.51	7.90	12.24	6.76	107.40	–	0.14	12	0.12	81
	03/09/2017	152	6.69	1.70	29.40	7.37	2.89	4.16	95.16	–	0.17	13	0.28	183
	10/09/2017	148	6.29	1.83	28.86	8.55	2.82	5.45	101.30	–	0.15	13	0.25	59
	16/09/2017	400	5.97	1.83	22.74	6.74	3.11	4.61	100.00	2.82	0.25	13	0.06	576
	17/09/2017	380	4.39	1.64	30.54	6.92	2.19	5.93	118.30	2.54	0.19	12	0.07	502
	24/09/2017	108	5.46	2.30	24.34	5.45	3.69	5.78	102.50	1.78	0.13	13	0.01	46
	01/10/2017	128	7.67	1.39	26.86	8.87	3.79	3.86	96.38	0.85	0.17	13	0.27	25
	08/10/2017	132	13.63	3.16	27.55	7.67	10.65	6.14	91.50	10.11	0.17	13	0.22	46
	22/10/2017	348	11.78	1.78	28.42	6.94	5.45	9.46	93.94	1.06	0.20	13	0.25	15
	05/11/2017	328	8.19	1.63	26.99	7.56	3.85	5.43	96.38	2.23	0.12	12	0.22	5
	12/11/2017	132	4.65	1.17	27.82	7.09	1.01	4.56	97.60	0.38	0.19	13	0.21	6
	19/11/2017	132	6.65	2.31	28.51	8.66	2.32	5.43	93.94	0.93	0.12	13	0.30	5
	26/11/2017	130	4.93	1.31	28.23	7.64	0.62	4.97	97.60	0.54	0.11	14	0.24	7
	03/12/2017	130	6.77	2.23	26.98	8.27	3.08	5.87	96.38	2.14	0.13	13	0.23	3
	10/12/2017	132	6.24	1.25	23.11	7.33	0.57	5.32	90.28	5.39	0.12	13	0.18	7
	17/12/2017	132	8.38	2.20	25.04	7.24	3.16	4.87	96.38	2.27	0.10	14	0.20	9
	24/12/2017	129	4.57	1.21	24.65	6.11	1.97	4.83	93.94	1.29	0.04	13	0.12	3
	30/12/2017	129	5.64	1.90	29.36	7.72	3.25	5.50	97.60	1.87	0.15	13	0.23	12
	21/01/2018	80	4.76	1.62	27.79	5.23	2.47	4.25	79.30	4.05	0.19	12	0.26	5
	28/01/2018	50	11.08	1.68	29.94	8.95	6.60	6.28	98.82	6.30	0.08	12	0.26	7
	04/02/2018	42	9.54	1.87	28.24	8.92	5.97	6.52	96.38	2.43	0.11	13	0.26	3
	04/03/2018	40	6.35	1.93	26.38	6.44	3.70	3.94	102.50	3.12	0.04	13	0.12	4
	11/03/2018	40	7.12	1.78	31.39	8.20	3.39	5.27	102.50	1.98	0.11	13	0.26	23
	01/04/2018	40	10.83	2.49	30.75	8.15	4.98	6.28	97.60	1.02	0.10	14	0.31	39
	08/04/2018	40	5.06	2.14	31.51	8.03	1.43	5.90	97.60	1.48	0.23	14	0.28	360
	16/04/2018	72	8.62	2.01	32.65	8.33	4.50	5.06	98.82	3.27	0.09	12	0.30	265
	29/04/2018	48	13.17	3.08	27.06	7.53	8.85	6.62	87.84	6.09	0.17	14	0.26	632
	06/05/2018	94	5.96	2.27	26.77	7.29	2.00	4.89	95.16	2.39	0.20	12	0.22	410
	13/05/2018	72	5.02	2.13	34.24	7.74	1.49	6.20	98.82	1.01	0.23	15	0.31	414
	27/05/2018	60	5.15	2.17	30.41	6.07	2.28	4.94	81.74	1.64	0.36	12	0.33	200
	03/06/2018	160	6.70	2.31	34.31	8.37	3.41	5.67	109.80	3.45	0.40	12	0.24	536
	17/06/2018	240	4.49	3.14	40.27	8.46	2.00	6.12	124.40	2.37	0.33	13	0.24	3727
	24/06/2018	87	4.29	1.47	35.91	8.02	0.94	5.25	112.20	0.96	0.11	12	0.25	338
	08/07/2018	72	5.25	1.64	28.60	7.51	1.23	2.62	103.70	0.31	0.12	12	0.22	197
	16/07/2018	160	5.59	2.78	23.19	5.50	3.88	5.97	106.10	2.57	0.08	12	– 0.05	387
	22/07/2018	2100	3.33	1.27	26.42	5.95	2.86	7.35	89.06	5.35	0.16	12	0.10	2310

Table 1 continued

Stations	Date	Discharge m ³ /s	Na ⁺ mg/l	K ⁺ mg/l	Ca ²⁺ mg/l	Mg ²⁺ mg/l	Cl ⁻ mg/l	SO ₄ ²⁻ mg/l	HCO ₃ ⁻ mg/l	NO ₃ ⁻ mg/l	PO ₄ ³⁻ mg/l	SiO ₂ mg/l	NIBC	TSS mg/l	
Dua	06/08/2017	869	4.16	1.75	23.39	4.35	2.68	2.87	84.18	–	0.20	12	0.13	77	
	14/08/2017	463	3.47	1.45	23.89	5.12	1.24	3.20	85.40	–	0.19	13	0.16	57	
	20/08/2017	860	8.65	1.97	23.04	4.84	5.47	3.88	63.44	–	0.13	12	0.35	106	
	27/08/2017	882	3.76	1.83	26.77	4.98	2.43	3.30	78.08	–	0.19	11	0.27	85	
	04/09/2017	565	3.99	1.54	21.73	5.23	2.30	3.29	70.76	–	0.15	12	0.25	58	
	10/09/2017	562	3.94	1.43	24.98	5.49	1.92	3.41	73.20	–	0.18	11	0.30	42	
	17/09/2017	2688	3.77	1.83	18.41	3.86	2.37	3.26	51.24	3.60	0.25	10	0.28	621	
	24/09/2017	610	4.59	2.10	23.47	5.39	2.06	4.11	75.64	3.35	0.15	12	0.23	62	
	01/10/2017	749	10.14	1.63	26.80	5.78	10.82	3.06	81.74	2.14	0.14	13	0.24	33	
	08/10/2017	1241	6.13	2.25	20.97	4.55	4.72	3.60	63.44	5.79	0.20	12	0.23	174	
	10/10/2017	1772	3.45	1.70	18.75	3.09	2.51	2.71	54.90	3.91	0.19	11	0.21	395	
	11/10/2017	3564	2.91	1.77	16.98	3.40	2.41	2.51	61.00	3.81	0.18	12	0.09	411	
	12/10/2017	4393	2.55	1.82	16.08	2.89	2.00	2.58	43.90	4.43	0.24	9	0.24	465	
	22/10/2017	700	8.65	1.76	26.22	6.37	5.06	5.68	78.08	3.78	0.17	14	0.29	40	
	05/11/2017	336	8.22	1.89	27.37	6.22	4.34	3.99	80.52	3.42	0.10	13	0.31	17	
	12/11/2017	440	9.51	2.30	27.86	6.68	5.99	4.34	84.18	3.12	0.16	14	0.30	8	
	20/11/2017	283	4.80	1.97	27.70	6.18	1.97	4.20	78.08	2.40	0.13	13	0.32	36	
	26/11/2017	246	3.73	1.45	24.71	5.30	0.97	4.21	80.52	2.38	0.14	14	0.21	17	
	03/12/2017	259	4.65	1.59	24.31	5.39	1.92	3.75	75.64	2.69	0.14	14	0.25	12	
	10/12/2017	494	4.28	1.57	23.88	5.30	1.71	3.73	84.18	3.00	0.11	13	0.16	10	
	18/12/2017	195	14.05	4.47	27.62	7.82	8.94	10.08	79.30	5.97	0.08	13	0.32	8	
	24/12/2017	170	4.98	1.45	24.14	5.45	2.22	4.41	81.74	2.08	0.09	13	0.20	4	
	31/12/2017	240	8.64	2.55	25.80	7.01	7.62	4.84	78.08	4.61	0.13	13	0.27	5	
	21/01/2018	289	5.66	1.59	27.85	6.08	2.45	4.00	81.70	1.95	0.12	11	0.30	9	
	27/01/2018	169	8.85	2.20	30.37	7.28	6.93	4.72	93.94	2.93	0.06	11	0.26	12	
	04/02/2018	154	4.37	1.51	28.35	6.04	1.23	4.37	86.62	1.42	0.14	13	0.27	8	
	04/03/2018	56	4.65	1.86	27.27	5.55	2.68	3.75	87.84	2.82	0.04	12	0.21	8	
	11/03/2018	185	4.43	1.62	30.77	6.45	1.53	4.56	87.84	1.97	0.13	12	0.30	8	
	02/04/2018	117	10.39	2.39	31.33	7.77	5.79	5.52	86.60	3.27	0.08	12	0.35	3	
	07/04/2018	345	4.50	1.62	31.64	6.29	2.37	4.45	86.62	1.64	0.08	12	0.31	139	
	17/04/2018	300	5.59	1.86	31.70	6.80	2.74	4.34	86.62	2.11	0.10	12	0.33	6	
	01/05/2018	275	4.31	1.92	28.14	5.79	2.10	4.34	80.52	1.81	0.09	13	0.29	14	
	06/05/2018	294	7.28	2.04	28.62	6.64	4.79	3.60	73.20	3.80	0.23	12	0.37	76	
	13/05/2018	339	8.69	2.21	27.00	5.59	5.69	4.66	74.42	4.46	0.19	12	0.31	44	
	20/05/2018	356	4.67	2.01	28.29	6.38	2.14	5.20	73.00	2.21	0.19	11	0.36	557	
	27/05/2018	252	4.38	2.03	29.49	5.64	2.09	3.05	76.86	1.05	0.20	11	0.35	9	
	03/06/2018	319	5.87	2.71	29.79	5.79	3.70	4.27	84.18	1.43	0.35	11	0.30	13	
	17/06/2018	316	6.95	2.37	27.14	5.46	4.99	4.70	73.20	2.63	0.13	13	0.31	157	
	24/06/2018	420	4.08	1.84	25.76	5.22	1.92	3.90	70.76	1.40	0.13	12	0.32	40	
	08/07/2018	455	8.85	2.34	30.31	6.70	4.82	5.43	84.18	2.30	0.19	12	0.33	13	
	16/07/2018	747	5.69	1.36	22.24	2.87	5.69	3.29	84.18	2.26	0.10	11	–	0.01	72
	22/07/2018	4210	2.22	1.79	20.71	4.30	1.26	4.58	70.76	3.83	0.26	11	0.11	867	

Table 1 continued

Stations	Date	Discharge m ³ /s	Na ⁺ mg/l	K ⁺ mg/l	Ca ²⁺ mg/l	Mg ²⁺ mg/l	Cl ⁻ mg/l	SO ₄ ²⁻ mg/l	HCO ₃ ⁻ mg/l	NO ₃ ⁻ mg/l	PO ₄ ³⁻ mg/l	SiO ₂ mg/l	NIBC	TSS mg/l
Yen Thuong	06/08/2017	752	3.39	1.44	21.74	4.15	1.51	3.27	74.42	-	-	-	0.17	158
	14/08/2017	430	3.39	1.60	22.97	4.69	1.72	3.20	86.62	-	0.23	12	0.10	77
	20/08/2017	862	3.97	1.72	18.73	4.19	1.98	2.91	62.22	-	0.13	11	0.24	187
	27/08/2017	750	4.80	1.97	24.02	4.46	3.65	3.56	68.32	-	0.25	11	0.29	117
	04/09/2017	475	3.80	1.82	24.77	4.27	3.02	3.03	65.88	-	0.14	11	0.31	107
	10/09/2017	514	3.83	1.58	25.53	4.98	2.29	3.56	68.32	-	0.14	12	0.33	66
	17/09/2017	2910	3.42	1.80	15.36	2.95	3.02	2.98	37.82	4.14	0.18	9	0.30	343
	18/09/2017	2625	6.42	1.80	18.03	2.48	5.34	2.29	50.02	5.28	0.20	10	0.22	369
	24/09/2017	750	5.26	2.17	17.98	4.73	3.59	4.11	53.68	3.68	0.13	12	0.28	85
	01/10/2017	690	5.16	1.91	27.33	5.17	4.23	3.72	75.64	2.57	0.15	12	0.28	95
	08/10/2017	2045	4.43	2.09	17.08	3.16	3.81	2.89	46.36	4.61	0.20	9	0.26	75
	10/10/2017	3150	2.58	2.17	15.29	2.60	2.58	3.10	36.60	4.08	0.25	8	0.29	200
	12/10/2017	4422	2.88	2.07	15.99	2.65	2.47	2.90	51.20	4.10	0.20	10	0.13	186
	22/10/2017	735	5.53	1.63	25.39	4.72	3.01	4.19	65.88	3.34	0.16	13	0.32	56
	05/11/2017	480	5.65	1.65	27.58	5.57	3.02	4.31	73.20	2.93	0.12	13	0.33	18
	12/11/2017	420	6.03	1.84	26.64	5.22	3.54	3.56	82.96	2.63	0.14	13	0.24	22
	20/11/2017	400	4.44	1.22	25.01	4.56	2.88	4.37	67.01	2.38	0.15	13	0.29	17
	27/11/2017	327	3.86	1.45	22.46	4.69	1.81	3.25	58.56	2.64	0.15	13	0.34	7
	03/12/2017	375	8.50	2.00	21.65	6.42	6.69	4.70	69.54	4.58	0.12	12	0.26	4
	10/12/2017	260	5.61	1.71	24.48	5.69	3.42	4.34	57.34	3.52	0.10	13	0.40	13
	18/12/2017	326	5.79	2.14	24.39	5.38	4.50	5.03	69.54	2.72	0.09	13	0.28	10
	24/12/2017	287	7.04	1.84	24.89	6.65	3.79	4.48	76.86	4.08	0.07	13	0.29	6
	31/12/2017	255	4.60	1.68	26.27	5.37	2.64	3.80	74.42	2.26	0.13	12	0.29	13
	21/01/2018	310	6.72	1.45	28.38	8.43	2.63	5.37	95.20	1.18	0.12	12	0.27	5
	27/01/2018	235	7.45	3.49	27.94	6.19	2.88	3.85	64.66	2.05	0.04	11	0.46	9
	04/02/2018	275	8.30	2.09	28.76	6.84	5.80	5.67	73.20	3.77	0.12	11	0.36	6
	04/03/2018	260	4.18	1.73	27.21	5.33	2.38	4.35	78.08	2.23	0.03	12	0.27	3
	11/03/2018	180	4.89	2.18	30.04	6.16	3.30	4.87	78.08	4.76	0.08	11	0.32	23
	02/04/2018	148	10.15	2.34	30.54	7.58	7.63	5.80	57.30	2.97	0.06	11	0.50	14
	07/04/2018	120	5.21	1.58	30.06	6.55	2.68	4.24	82.96	2.09	0.11	12	0.32	18
	17/04/2018	142	4.72	1.85	29.25	6.25	1.88	4.05	73.20	1.92	0.20	13	0.38	7
	06/05/2018	119	8.91	2.17	23.71	5.69	6.59	4.78	62.22	5.48	0.25	11	0.33	211
	13/05/2018	335	6.60	2.05	27.64	5.50	4.01	4.61	73.20	3.64	0.25	12	0.32	55
	20/05/2018	180	5.29	2.87	27.21	5.81	2.66	5.58	62.00	2.82	0.21	12	0.41	33
	28/05/2018	176	7.10	2.30	31.14	7.70	3.69	8.85	93.94	2.04	0.22	10	0.27	25
	02/06/2018	149	5.22	2.05	27.49	5.51	2.62	3.80	74.42	2.13	0.25	12	0.33	13
	17/06/2018	240	11.81	3.21	28.47	8.15	9.51	8.73	73.20	3.16	0.21	13	0.36	12
	24/06/2018	370	5.07	1.78	24.02	5.48	2.26	4.20	75.64	0.90	0.11	12	0.26	24
	08/07/2018	300	5.25	2.16	28.80	6.26	2.44	4.28	81.74	1.28	0.25	12	0.32	52
	16/07/2018	350	3.35	1.82	22.31	4.34	2.93	5.47	65.88	1.70	0.09	10	0.21	246
	22/07/2018	1410	2.32	1.24	18.13	3.27	1.37	5.56	54.90	5.95	0.13	10	0.12	228

241 month to month (Fig. 3), showing the opposite trend of that
 242 seen for solute concentration, except at My Ly (for
 243 example, in June and July). The highest SSCs occurred
 244 during September, October, and July at Dua and Yen

Thuong (135–317 mg/L). Peak SSC occurred in June at
 My Ly (1534 mg/L), indicating significant erosion in the
 upper basin due to heavy rain.

245
 246
 247

Fig. 2 Seasonal variations in the concentration of major ions (μM), TDS, and SS (mg/l)

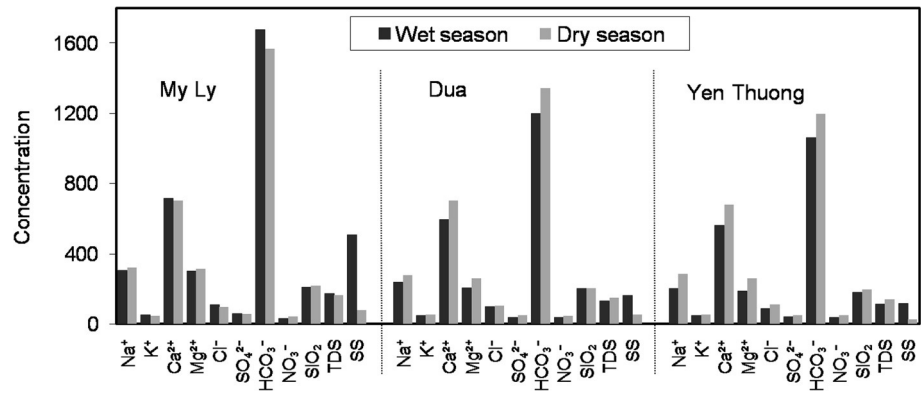
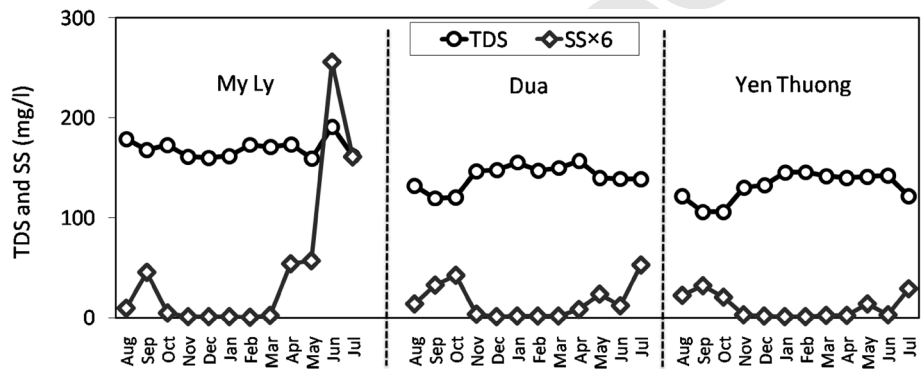


Fig. 3 Monthly variations in the concentration of TDS and SS (mg/l)



248 4.3 Weathering processes controlling the major ion 249 chemistry

250 Major natural processes determining the ion chemistry of
251 water can be identified by plotting variations in the weight
252 ratio between Na^+ and $\text{Na}^+ + \text{Ca}^{2+}$ as a function of TDS
253 (Gibbs 1970). The sources of major ions were divided into
254 three groups: precipitation dominance, rock dominance,
255 and evaporation-crystallization dominance. Figure 4 shows
256 weathering dominance for most of the samples drawn.
257 Rock weathering controls the water composition in the Ca
258 River basin, producing a TDS value between 77 and
259 205 mg/L and a $\text{Na}^+ / (\text{Na}^+ + \text{Ca}^{2+})$ ratio ranging from
260 0.10 to 0.43.

261 The three primary lithologies undergoing chemical
262 weathering were silicates, carbonates, and evaporites
263 (Gaillardet et al. 1997). Carbonate weathering (calcite,
264 dolomites) produces Ca^{2+} , Mg^{2+} , and HCO_3^- . Silicate
265 weathering results in HCO_3^- , Na^+ , K^+ , Mg^{2+} , Ca^{2+} , and
266 SiO_2 . Evaporite dissolution results in Na^+ , K^+ , Cl^- , and
267 SO_4^{2-} (Han and Liu 2001; Meybeck 1987; Sarin et al.
268 1989). The relationships between $\text{Ca}^{2+}/\text{HCO}_3^-$,
269 $(\text{Ca}^{2+} + \text{Mg}^{2+})/\text{total cations}$, and $(\text{Na}^+ + \text{K}^+)/\text{total cations}$
270 for the Ca River were determined to evaluate the contri-
271 bution of rock weathering. The Ca^{2+} and HCO_3^- for most
272 samples fell along a 1:1 equiline (Fig. 5a), implying that

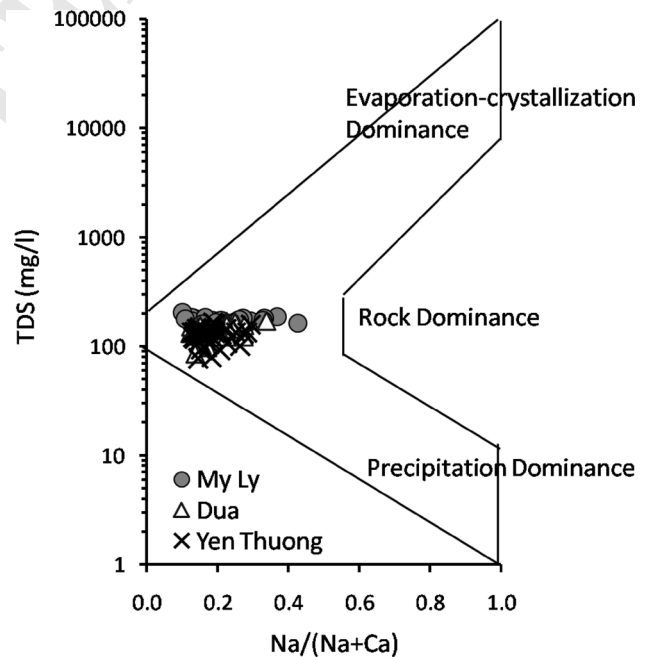


Fig. 4 The Gibbs graph of Ca River between the ratio of $\text{Na}/(\text{Na} + \text{Ca})$ and total dissolved solids

273 carbonates dissolution dominates in this drainage basin
274 (Roy et al. 1999). The HCO_3^- is slightly more enriched than
275 Ca^{2+} at My Ly, possibly consistent with a silicate weath-
276 ering source for some of this anion (Holland 1978). The



277 scatter plot (Fig. 5b) of $(Ca^{2+} + Mg^{2+})$ against total
 278 cations indicates a significant contribution of these two
 279 cations (approximately 85% of the total). Any deviation of
 280 $(Ca^{2+} + Mg^{2+})$ from the 1:0.85 line was attributed to
 281 increasing proportions of $(Na^{+} + K^{+})$ (Fig. 5b, c), implying
 282 contributions from silicate weathering or evaporite disso-
 283 lution (Li and Zhang 2008; Maharana et al. 2015). The
 284 correlations among geochemistry parameters and their
 285 correlations with suspended solids were investigated for
 286 each station (Table 2). The significant relationships
 287 between Ca^{2+}/Mg^{2+} , Ca^{2+}/HCO_3^- , Mg^{2+}/HCO_3^- ,
 288 Ca^{2+}/TDS , Mg^{2+}/TDS , and HCO_3^-/TDS at all stations
 289 support the finding of carbonate weathering dominance in
 290 the Ca River basin. Significant correlations between SiO_2
 291 and Na^{+} , K^{+} , or HCO_3^- were not found, implying minimal
 292 silicate weathering. However, moderate correlations
 293 between Cl^- , SO_4^{2-} , Na^{+} , K^{+} , and TDS were found,
 294 indicating that evaporite weathering was the source (Li and
 295 Zhang 2008).

The Piper diagram is widely applied to determine the
 296 classification of water on the basis of its chemical character
 297 (Maharana et al. 2015; Negrel et al. 2007; Ji and Jiang
 298 2012). The triangular cationic fields of the Piper diagram
 299 (Fig. 6) revealed that most of the water samples fell into
 300 the Ca^{2+} field, whereas in the anion triangle, the majority
 301 fell into the HCO_3^- field. Chemical data plotted on the
 302 diamond-shaped central field revealed the dominance of
 303 the $Ca^{2+} - HCO_3^-$ type. Therefore, $Ca^{2+} - HCO_3^-$ is the
 304 dominant hydrogeochemical species in the Ca River basin.
 305 The Piper diagram for our Ca River samples is similar to
 306 that for the Son River (Maharana et al. 2015) and the
 307 upstream Huanghe River (Fan et al. 2014), dominated by
 308 carbonate weathering. However, it differs from the mid-
 309 and downstream sections of the Huanghe River (Fan et al.
 310 2014), where evaporite dissolution dominates. They also
 311 differ from the Liao River, Daling River, Hun-Tai River
 312 (Ding et al. 2016), Ou River, and Min River (Liu et al.
 313 2018), where silicate weathering dominates. In many
 314

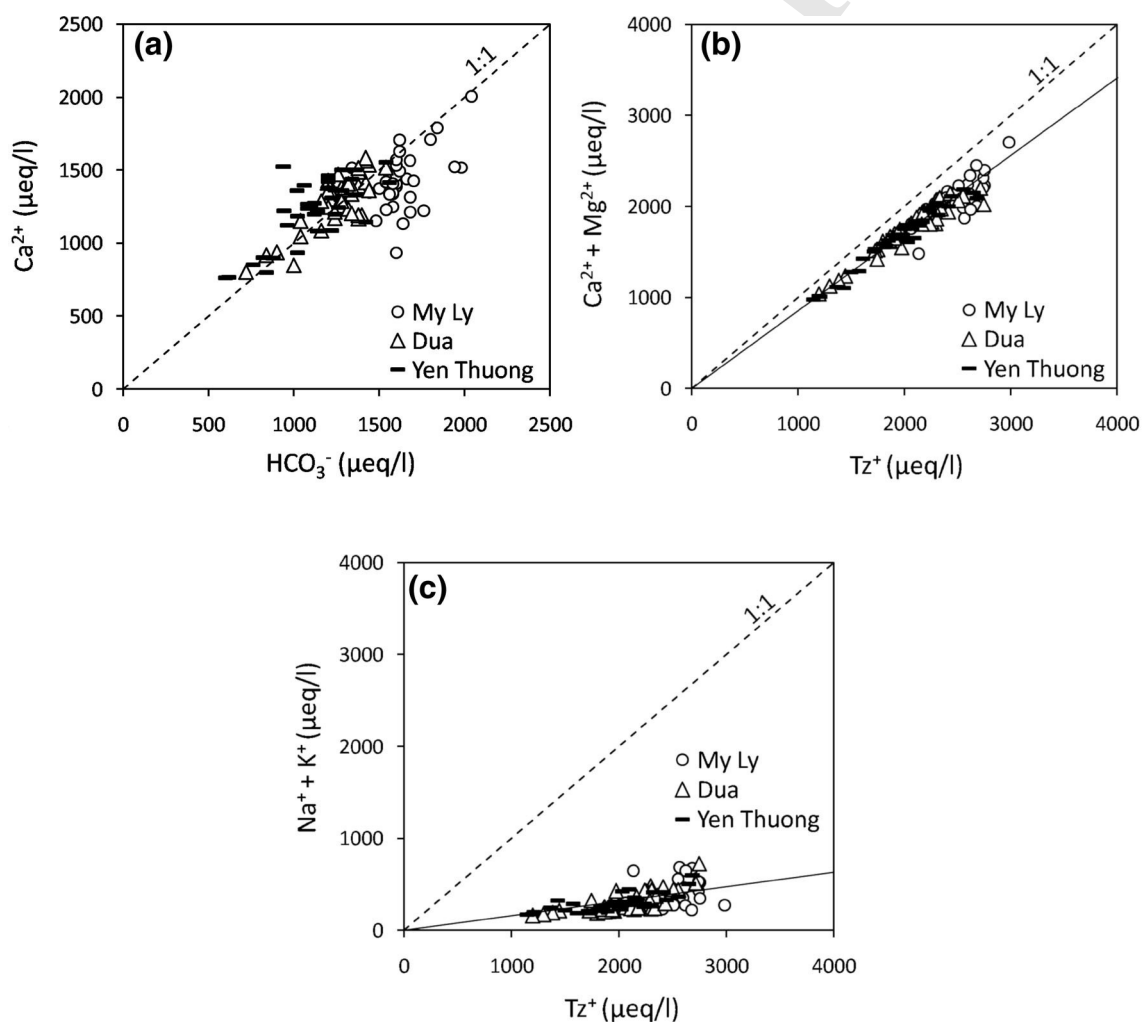


Fig. 5 Scatter plots between **a** Ca^{2+} and HCO_3^- , **b** Ca^{2+} , Mg^{2+} , and total cations, and **c** Na^{+} , K^{+} , and total cations

Table 2 Correlation matrix of measured parameters at three hydrological stations

	Na ⁺	K ⁺	Ca ²⁺	Mg ²⁺	Cl ⁻	SO ₄ ²⁻	HCO ₃ ⁻	NO ₃ ⁻	PO ₄ ³⁻	SiO ₂	TDS	TSS
<i>My Ly</i>												
Na ⁺	1.00											
K ⁺	0.43**	1.00										
Ca ²⁺	0.30	0.16	1.00									
Mg ²⁺	0.26	0.11	0.48**	1.00								
Cl ⁻	0.91**	0.54**	-0.30	0.11	1.00							
SO ₄ ²⁻	0.44**	0.33*	0.04	0.05	0.46**	1.00						
HCO ₃ ⁻	-0.19	0.10	0.42**	0.30	-0.13	-0.04	1.00					
NO ₃ ⁻	0.49**	0.34	-0.17	-0.04	0.67**	0.24	-0.25	1.00				
PO ₄ ³⁻	-0.15	0.27	0.40**	0.01	-0.10	0.12	0.06	0.00	1.00			
SiO ₂	0.12	0.17	0.01	0.17	-0.03	0.15	-0.19	-0.16	-0.04	1.00		
TDS	0.33*	0.49**	0.54**	0.55**	0.37*	0.34*	0.76**	0.18	0.15	-0.03	1.00	
TSS	-0.27	0.28	0.43**	-0.01	-0.12	0.23	0.35*	0.13	0.44**	-0.07	0.36*	1.00
<i>Dua</i>												
Na ⁺	1.00											
K ⁺	0.68**	1.00										
Ca ²⁺	0.45**	0.25	1.00									
Mg ²⁺	0.64**	0.47**	0.85***	1.00								
Cl ⁻	0.89**	0.56**	0.22	0.37*	1.00							
SO ₄ ²⁻	0.67**	0.77**	0.46**	0.68**	0.41**	1.00						
HCO ₃ ⁻	0.31*	0.03	0.78**	0.65**	0.16	0.33*	1.00					
NO ₃ ⁻	0.35*	0.49**	-0.47**	-0.10	0.39*	0.28	-0.47**	1.00				
PO ₄ ³⁻	-0.30	0.00	-0.35*	-0.39*	-0.20	-0.30	-0.48**	0.13	1.00			
SiO ₂	0.35*	0.06	0.28	0.43**	0.19	0.32*	0.45**	-0.03	-0.41**	1.00		
TDS	0.69**	0.40**	0.86**	0.86**	0.50**	0.62**	0.88**	-0.19	-0.49**	0.51**	1.00	
TSS	-0.42**	-0.10	-0.59**	-0.53**	-0.25	-0.18	-0.66**	0.28	0.49**	-0.53**	-0.66**	1.00
<i>Yen Thuong</i>												
Na ⁺	1.00											
K ⁺	0.56**	1.00										
Ca ²⁺	0.50**	0.23	1.00									
Mg ²⁺	0.73**	0.34*	0.84**	1.00								
Cl ⁻	0.87**	0.50**	0.19	0.41**	1.00							
SO ₄ ²⁻	0.60**	0.39*	0.53**	0.71**	0.49**	1.00						
HCO ₃ ⁻	0.25	-0.09	0.76**	0.70**	-0.06	0.40**	1.00					



Table 2 continued

	Na ⁺	K ⁺	Ca ²⁺	Mg ²⁺	Cl ⁻	SO ₄ ²⁻	HCO ₃ ⁻	NO ₃ ⁻	PO ₄ ³⁻	SiO ₂	TDS	TSS
NO ₃ ⁻	0.02	- 0.03	- 0.55**	- 0.45**	0.31	- 0.16	- 0.58**	1.00				
PO ₄ ³⁻	- 0.08	0.09	- 0.19	- 0.24	0.02	- 0.06	- 0.12	0.16	1.00			
SiO ₂	0.29	- 0.13	0.55**	0.51**	0.04	0.15	0.54**	- 0.41*	- 0.23	1.00		
TDS	0.59**	0.16	0.90**	0.89**	0.28	0.63**	0.92**	- 0.48**	- 0.15	0.59**	1.00	
TSS	- 0.37*	- 0.17	- 0.72**	- 0.72**	- 0.07	- 0.36*	- 0.60**	0.51**	0.30	- 0.69**	- 0.69**	1.00

**Correlation is significant at the 0.01 level

*Correlation is significant at the 0.05 level

watersheds around the world, carbonate weathering play an important role in controlling river water chemistry because carbonate is more susceptible to weathering than silicate (Fan et al. 2014; Roy et al. 1999).

4.4 Variations in major solute concentrations at discharge

The relationships between solute concentration and its discharge were investigated at each hydrological station. Concentrations of the weathering-derived solutes were plotted against instantaneous discharge on logarithmic axes (Fig. 7), yielding the approximate relationships between concentration and discharge using a power law (Barons et al. 2017; Herndon et al. 2015; Musolff et al. 2015):

$$C = a \times Q^b \quad (1)$$

where C is solute concentration, Q is discharge, and a and b are constants. The exponent b is the slope of the $C - Q$ relationship on logarithmic axes. When concentration does not change with changing discharge, the relationship is said to be chemostatic (Moatar et al. 2017; Musolff et al. 2015). When this is the case, b is between -0.1 and 0 (Herndon et al. 2015; Hunsaker and Johnson 2017). When discharge increases, solute concentrations can either increase (enrichment behavior, $b > 0$) or decrease (dilution behavior, $b < -0.1$), and the relationship is said to be chemodynamic (Herndon et al. 2015).

Our results show that the upstream catchment (My Ly) behaved chemostatically for the major chemical weathering products except for Na⁺ ($b = -0.11$), NO₃⁻ ($b = 0.11$), and PO₄³⁻ ($b = 0.15$). The large store/high production rate of weathering products can lead to chemostatic behavior for major ions (Musolff et al. 2015). Nutrient increases with increasing discharge at My Ly indicated the source was organic matter degradation in the forest area. Similar trends for the major ions at discharge were seen at Dua and Yen Thuong. Negative slopes were found for Ca²⁺, Mg²⁺, and HCO₃⁻ ($b = -0.12$ to -0.28) with low variability ($R^2 \geq 0.5$) and for Na⁺ and SO₄²⁻ ($b = -0.13$ to -0.22) with moderate variability ($R^2 \geq 0.3$). The concentrations of NO₃⁻ and PO₄³⁻ were constant or increasing, indicating enrichment in nutrient sources in the basin (Musolff et al. 2015). Meanwhile, K⁺ and Cl⁻ behaved chemostatically, increasing in the discharge at all basins, indicating important biogeochemical influences (Saunders and Lewis 1989) or exogenous sources (atmospheric deposition) (Musolff et al. 2015). For the major solutes (Ca²⁺, Mg²⁺, Na⁺, and HCO₃⁻), the dilution slopes at the downstream station were greater than those found midstream, indicating that catchments with higher water yields were more likely to express dilution (Moatar et al. 2017). The negative

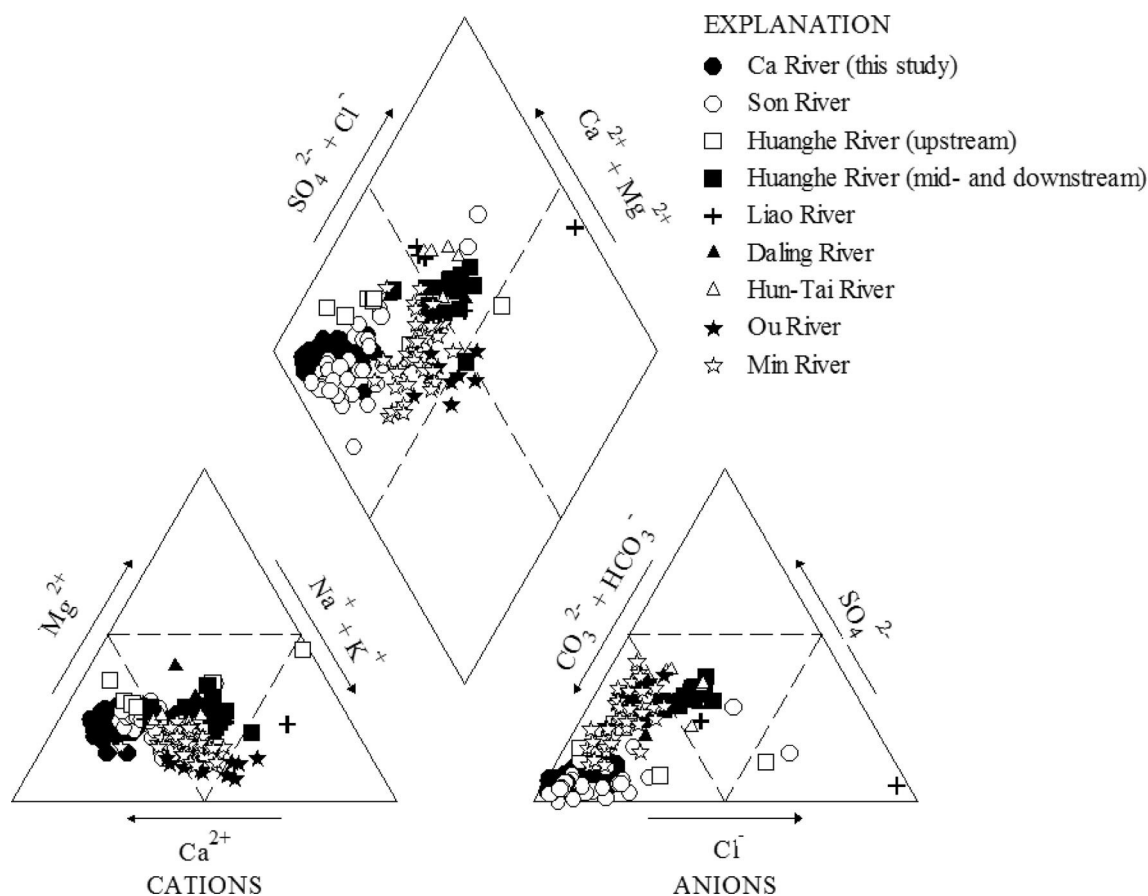


Fig. 6 Piper trilinear diagram of Ca River water in comparison with other river basins (data from Ding et al. 2016; Fan et al. 2014; Liu et al. 2018; Maharana et al. 2015)

364 correlation between major elements and runoff increased
 365 (higher R^2 values) with decreasing elevation (Torres et al.
 366 2015). Less-reactive elements (Ca^{2+} , Mg^{2+} , and HCO_3^-)
 367 exhibited strong correlations with discharge and indicated
 368 various degrees of dilution with increasing runoff (Baronas
 369 et al. 2017). However, low correlations found for PO_4^{3-} ,
 370 NO_3^- , Cl^- , and K^+ reflected biological processes, atmo-
 371 spheric input, or anthropogenic impacts (i.e., fertilizer
 372 application) (Bluth and Kump 1994; Moatar et al. 2017).

373 4.5 Primary evidence of reservoir impact 374 on concentrations of suspended solids 375 and dissolved solids

376 Located above the largest reservoir of the Ca River basin,
 377 My Ly is significantly influenced by the operation of the
 378 Ban Ve reservoir. The impact of water storage at the Ban
 379 Ve reservoir on the correlation between SSC and discharge
 380 at My Ly is shown in Fig. 8a. In August and September
 381 (the rainy season), SSC increased with increasing dis-
 382 charge. Water storage starts at the end of the rainy season
 383 (October), leading to increased water levels behind the

reservoir. The water level was raised until it was over the 384
 My Ly station. Consequently, runoff was delayed during 385
 November and December. As a result, the SSC gradually 386
 decreased as suspended sediment settled, and sediment 387
 suspension was deferred during this period. The reservoir 388
 opened at the beginning of January, but SSC remained low 389
 until March because it was the dry season. Rain in April 390
 and May can wash out the settled sediment surrounding the 391
 upper part of My Ly, resulting in the steep increases in 392
 SSC. Thereafter, SSC increases with increasing discharge 393
 in June and July, consistent with increases seen in August 394
 and September. 395

Dua and Yen Thuong, located in the lower part of the 396
 main reservoirs in the Ca River basin, showed similar SSC 397
 behaviors in their discharges (Fig. 8b, c): decreasing SSCs 398
 with increasing discharge when comparing the rainy to dry 399
 seasons. This reflects the impact of suspended sediment 400
 settling in the reservoirs. Upstream sediment erosion also 401
 influenced that seen downstream; this is implied by the 402
 high SSC found in May. Generally, SSCs are positively 403
 correlated with streamflow (Moore and Anderholm 2002). 404

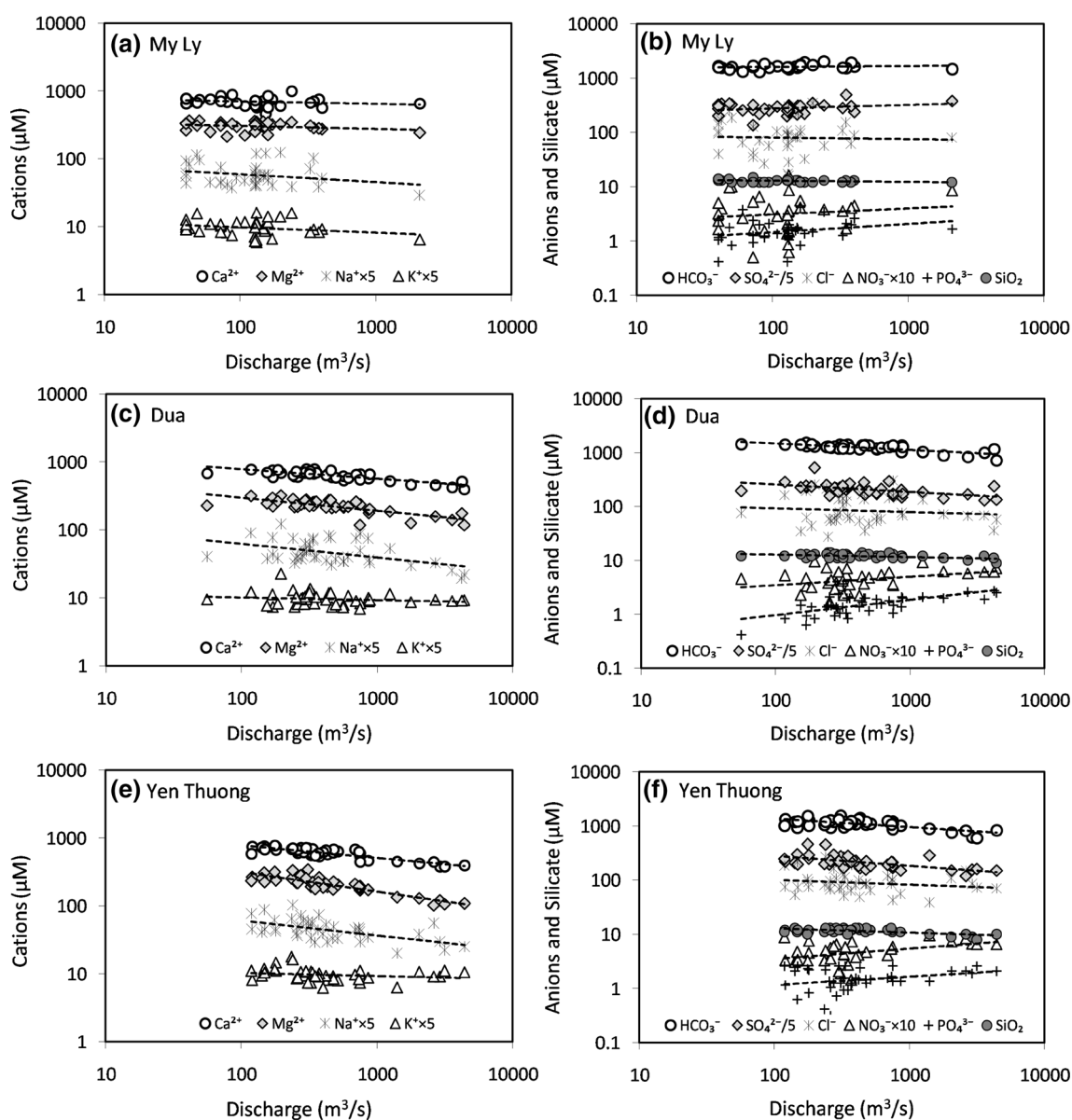


Fig. 7 Variation of river elements concentration with discharge at My Ly (a, b), Dua (c, d), and Yen Thuong (e, f)

405 However, reservoir operations lead to a variety of SSC
406 behaviors in the discharge.

407 Dam closure not only affects suspended sediment but
408 also river water quality (Muigai et al. 2010; Castilla-Her-
409 nandez et al. 2014). Variations in solute concentrations
410 with discharge at My Ly were quite different from the
411 fluxes with discharge at Dua and Yen Thuong. Differences
412 could be the results of the impacts of the reservoir. During
413 the wet season, when water is stored at My Ly, most ion
414 concentrations were less variated than in other periods.
415 When the reservoir was open, ion concentrations increased
416 with discharge during the dry season until the highest
417 concentration was reached at the first flash flood on 17 June
418 2018. Since then, ion concentrations decreased due to

dilution. However, inverse correlations between ion con- 419
centrations and discharges were seen at Dua and 420
Yen Thuong, indicating dilution effects (Zhang et al. 2015). 421
When discharge exceeded 1000 m³/s, ion concentrations 422
decreased sharply, for example, on 17 December 2017, 8– 423
12 October 2017, and 22 July 2018. The correlations 424
between TSS and geochemical parameters are shown in 425
Table 2 and indicate that suspended solids are negatively 426
correlated with all ions (except NO₃⁻ and PO₄³⁻) and TDS at 427
Dua and Yen Thuong. This is common with increases in 428
sediment, whereas chemical ions become diluted with 429
increasing discharge. In contrast, positive correlations 430
between TSS and K⁺, Ca²⁺, SO₄²⁻, HCO₃⁻, NO₃⁻, PO₄³⁻, 431
and TDS were identified at My Ly. These results imply a 432

433 significant geochemical impact of water storage in the My
 434 Ly basin. When the water level at My Ly rises, My Ly can
 435 act as a reservoir, resulting in sediment suspension and
 436 sediment settling. Dam closures lead to increased water
 437 residence time, causing increased interaction between
 438 sediment particles and solutes. Dam closures also change
 439 the environmental water conditions (low oxygen content
 440 and high temperature), favoring biogeochemical processes
 441 (Moatar et al. 2017). Muigai et al. (2010) indicated that the
 442 reservoir leads to decreases in dissolved oxygen content
 443 due to eutrophication and increases the TDS value. Moore
 444 and Anderholm (2002) found that, in downstream reser-
 445 voirs, TDS concentrations increase from evapotranspiration
 446 while nutrient concentrations decrease from settling
 447 and nutrient uptake, and SSCs decrease due to settling. In
 448 this study, it was not easy to assess the impact of the
 449 reservoir on the downstream basin because TDS values
 450 showed small seasonal variations. Moreover, the TDS
 451 concentration and composition were significantly influ-
 452 enced by multiple factors such as human activity,
 453 groundwater discharge, and tributary inflow. Therefore, the
 454 impact of dam closure on TDS in the downstream basin
 455 requires further investigation.

456 5 Conclusions

457 From 121 Ca River water samples collected from August
 458 2017 to July 2018 at three stations, cations (Ca^{2+} , Mg^{2+} ,
 459 Na^+ , and K^+), anions (HCO_3^- , SO_4^{2-} , Cl^- , NO_3^- , and
 460 PO_4^{3-}), dissolved silica, SSCs, and TDS values showed that
 461 carbonate weathering is dominant. Bicarbonate and calcium
 462 are the prevailing chemical species, accounting for
 463 84.4% and 62.0% of the total anionic and cationic charges,
 464 respectively. The TDS values varied from 77 to 205 mg/L,
 465 averaging 144 mg/L and decreasing in the downstream
 466 basin with decreases in major solute concentrations.

467 The relationships between solute concentrations and
 468 discharge show that the upstream catchment (My Ly)
 469 behaves chemostatically for the major chemical weathering
 470 products. Similar negative trends for Ca^{2+} , Mg^{2+} , HCO_3^- ,
 471 Na^+ , and SO_4^{2-} with discharge at Dua and Yen Thuong
 472 indicate dilution behaviors for those ions. The constant or
 473 increasing ion concentrations of NO_3^- and PO_4^{3-} in the
 474 three basins reflect enrichment of nutrients from organic
 475 matter degradation or human activity.

476 Relationships between SSC and discharge show that the
 477 reservoirs along the Ca River trigger sediment suspension
 478 and sediment settling at the My Ly station and decreasing
 479 SSCs at the Dua and Yen Thuong stations. Delays in water
 480 flow can lead to greater interactions between sediment and
 481 solutes and can allow biogeochemical processes that result

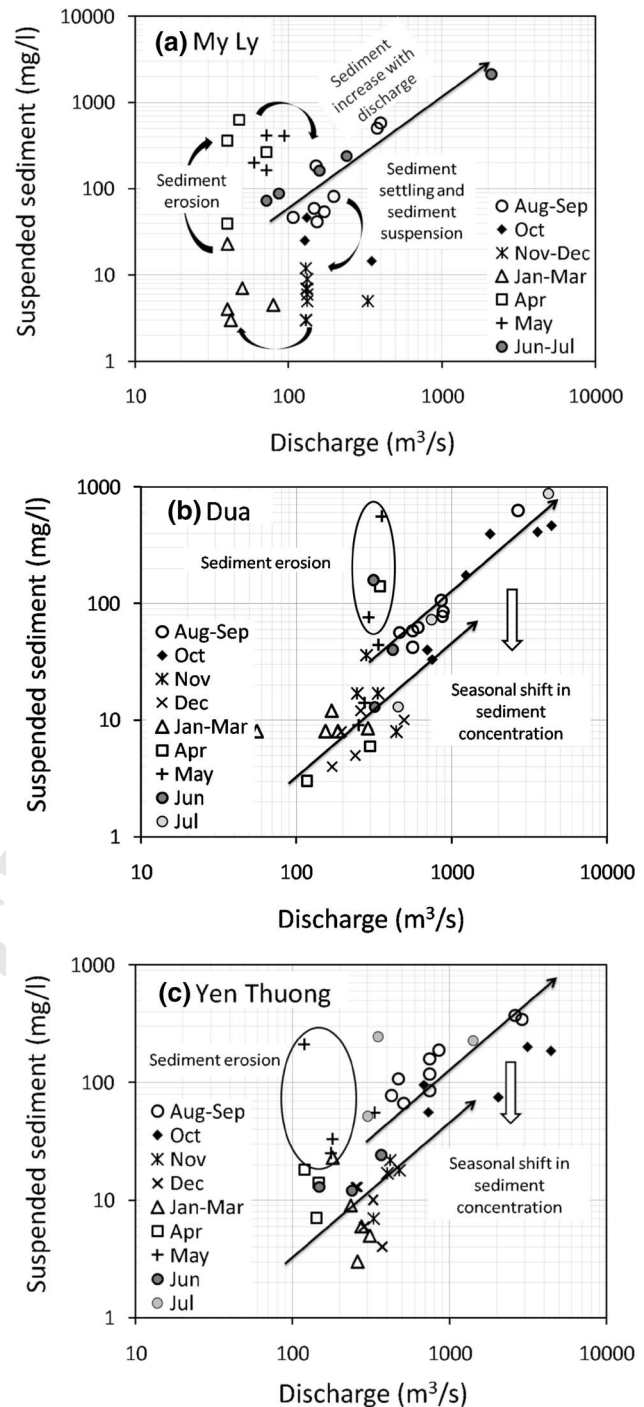


Fig. 8 Variation of suspended sediment concentration with discharge at My Ly (a), Dua (b) and Yen Thuong (c)

in unusual changes in the concentrations of major ions and
 TDS with increasing discharges at My Ly.

Acknowledgements This research was financially supported by the
 Japan Society for the Promotion of Science (Grant no. R11604). The
 authors would like to express their deep appreciation to Dr. Mitsuyo
 Saito of Graduate School Environmental and Life Science, Okayama
 University for her helpful comments on the manuscript and kind

489 support through the research process. The authors also thank staffs of
490 North-Central Hydro-meteorological Centre, Vietnam for allowing us
491 access to their gauging records. An anonymous reviewer is thanked
492 for critically reading the manuscript and suggesting substantial
493 improvements.

494 References

495 Amos P, Veale B, Thai NC, Read S (2017) Improving dam and
496 downstream community safety in Vietnam. *Hydropower Dams*
497 1:37–43

498 Baronas JJ, Torres MA, Clark KE, West AJ (2017) Mixing as a driver
499 of temporal variations in river hydrochemistry: 2. Major and
500 trace element concentration dynamics in the Andes-Amazon
501 transition. *Water Resour Res* 53(4):3120–3145. [https://doi.org/](https://doi.org/10.1002/2016WR019729)
502 [10.1002/2016WR019729](https://doi.org/10.1002/2016WR019729)

503 Bluth GJS, Kump LR (1994) Lithologic and climatologic controls of
504 river chemistry. *Geochim Cosmochim Acta* 58(10):2341–2359.
505 [https://doi.org/10.1016/0016-7037\(94\)90015-9](https://doi.org/10.1016/0016-7037(94)90015-9)

506 Bruijnzeel LA (1983) Hydrological and biogeochemical aspects of
507 man-made forests in south-central Java, Indonesia. PhD Thesis,
508 Vrije Universiteit, Amsterdam, p 256

509 Castilla-Hernandez P, del del R Torres-Alvarado M, Herrera-San Luis
510 JA, Cruz-Lopez N (2014) Water quality of a reservoir and its
511 major tributary located in east-central Mexico. *Int J Environ Res*
512 *Public Health* 11(6):6119–6135. [https://doi.org/10.3390/](https://doi.org/10.3390/ijerph110606119)
513 [ijerph110606119](https://doi.org/10.3390/ijerph110606119)

514 Chetelat B, Liu C-Q, Zhao ZQ, Wang QL, Li SL, Li J, Wang BL
515 (2008) Geochemistry of the dissolved load of the Changjiang
516 Basin rivers: anthropogenic impacts and chemical weathering.
517 *Geochim Cosmochim Acta* 72(17):4254–4277. [https://doi.org/](https://doi.org/10.1016/j.gca.2008.06.013)
518 [10.1016/j.gca.2008.06.013](https://doi.org/10.1016/j.gca.2008.06.013)

519 Chikamori H, Heng L, Daniel T (eds) (2012) Catalogue of rivers for
520 Southeast Asia and the Pacific–Volume VI. UNESCO-IHP
521 Regional Steering Committee for Southeast Asia and the Pacific.
522 <http://unesdoc.unesco.org/images/0021/002170/217039e.pdf>

523 Ding H, Liu C-Q, Zhao Z-Q, Li S-L, Lang Y-C, Li X-D, Hu J, Liu B-J
524 (2016) Geochemistry of the dissolved loads of the Liao River
525 basin in northeast China under anthropogenic pressure: chemical
526 weathering and controlling factors. *J Asian Earth Sci*
527 138:657–671. <https://doi.org/10.1016/j.jseaes.2016.07.026>

528 Fan B-L, Zhao Z-Q, Tao F-X, Liu B-J, Tao Z-H, Gao S, Zhang L-H
529 (2014) Characteristics of carbonate, evaporite and silicate
530 weathering in Huanghe River basin: a comparison among the
531 upstream, midstream and downstream. *J Asian Earth Sci*
532 96:17–26. <https://doi.org/10.1016/j.jseaes.2014.09.005>

533 Gaillardet J, Dupre B, Allegre CJ, Negrel P (1997) Chemical and
534 physical denudation in the Amazon River Basin. *Chem Geol*
535 142(3–4):141–173. [https://doi.org/10.1016/s0009-2541\(97\)00074-0](https://doi.org/10.1016/s0009-2541(97)00074-0)

536 Gibbs RJ (1970) Mechanisms controlling world water chemistry.
537 *Science* 170(3962):1088–1090. [https://doi.org/10.1126/science.](https://doi.org/10.1126/science.170.3962.1088)
538 [170.3962.1088](https://doi.org/10.1126/science.170.3962.1088)

539 Godsey SE, Kirchner JW, Clow DW (2009) Concentration–discharge
540 relationships reflect chemostatic characteristics of US catch-
541 ments. *Hydrol Process* 23(13):1844–1864. [https://doi.org/10.](https://doi.org/10.1002/hyp.7315)
542 [1002/hyp.7315](https://doi.org/10.1002/hyp.7315)

543 Han G, Liu C (2001) Hydrogeochemistry of Wujiang River water in
544 Guizhou province China. *Chin J Geochem* 20(3):240–248.
545 <https://doi.org/10.1007/BF03166145>

546 Herndon EM, Dere AL, Sullivan PL, Norris D, Reynolds B, Brantley
547 SL (2015) Landscape heterogeneity drives contrasting concentra-
548 tion–discharge relationships in shale headwater catchments.
549 *Hydrol Earth Syst Sci* 19:3333–3347. [https://doi.org/10.5194/](https://doi.org/10.5194/hess-19-3333-2015)
550 [hess-19-3333-2015](https://doi.org/10.5194/hess-19-3333-2015)

Holland HD (1978) The chemistry of the atmosphere and oceans. 551
Wiley, Hoboken, p 351 552

Hunsaker CT, Johnson DW (2017) Concentration-discharge relation- 553
ships in headwater streams of the Sierra Nevada, California. 554
Water Resour Res 53(9):7869–7884. [https://doi.org/10.1002/](https://doi.org/10.1002/2016WR019693) 555
[2016WR019693](https://doi.org/10.1002/2016WR019693) 556

IWRP (2012) Synthesis report of “Review of water resources planning in 557
the Ca River basin” (in Vietnamese). Institute of Water Resources 558
Planning, Directorate of Water Resources, Ha Noi 559

Ji H, Jiang Y (2012) Carbon flux and C, S isotopic characteristics of 560
river waters from a karstic and a granitic terrain in the Yangtze 561
River system. *J Asian Earth Sci* 57:38–53. [https://doi.org/10.](https://doi.org/10.1016/j.jseaes.2012.06.004) 562
[1016/j.jseaes.2012.06.004](https://doi.org/10.1016/j.jseaes.2012.06.004) 563

Li S, Zhang Q (2008) Geochemistry of the upper Han River basin, 564
China, 1: spatial distribution of major ion compositions and their 565
controlling factors. *Appl Geochem* 23(12):3535–3544. [https://](https://doi.org/10.1016/j.apgeochem.2008.08.012) 566
doi.org/10.1016/j.apgeochem.2008.08.012 567

Li S, Xu Z, Wang H, Wang J, Zhang Q (2009) Geochemistry of the 568
upper Han River basin, China 3: anthropogenic inputs and 569
chemical weathering to the dissolved load. *Chem Geol* 570
264(1–4):89–95. <https://doi.org/10.1016/j.chemgeo.2009.02.021> 571

Liu W, Xu Z, Sun H, Zhao T, Shi C, Liu T (2018) Geochemistry of 572
the dissolved loads of rivers in Southeast Coastal Region, China: 573
anthropogenic impact on chemical weathering and carbon 574
sequestration. *Biogeosci Discuss.* [https://doi.org/10.5194/bg-](https://doi.org/10.5194/bg-2018-109) 575
[2018-109](https://doi.org/10.5194/bg-2018-109) (in review) 576

Maharana C, Gautam SK, Singh AK, Tripathi JK (2015) Major ion 577
chemistry of the Son River, India: weathering processes, 578
dissolved fluxes and water quality assessment. *J Earth Syst Sci* 579
124(6):1293–1309. <https://doi.org/10.1007/s12040-015-0599-0> 580

Meybeck M (1987) Global chemical weathering of surficial rocks 581
estimated from river dissolved loads. *Am J Sci* 287(5):401–428. 582
<https://doi.org/10.2475/ajs.287.5.401> 583

Meybeck M (1994) Origin and variable composition of present day 584
riverborne material. *Material Fluxes on the Surface of the Earth.* 585
National Academic Press, Washington, DC, pp 61–73 586

Meybeck M, Helmer R (1989) The quality of rivers: from pristine 587
stage to global pollution. *Palaeogeogr Palaeoclimatol Palaeoecol* 588
75(4):283–309. [https://doi.org/10.1016/0031-0182\(89\)90191-0](https://doi.org/10.1016/0031-0182(89)90191-0) 589

Milliman JD, Farnsworth KL (2011) River discharge to the coastal 590
ocean: a global synthesis. Cambridge University Press, Cam- 591
bridge, p 384. <https://doi.org/10.1017/CBO9780511781247> 592

Moatar F, Abbott BW, Minaudo C, Curie F, Pinay G (2017) 593
Elemental properties, hydrology, and biology interact to shape 594
concentration-discharge curves for carbon, nutrients, sediment, 595
and major ions. *Water Resour Res* 53(2):1270–1287. [https://doi.](https://doi.org/10.1002/2016WR019635) 596
[org/10.1002/2016WR019635](https://doi.org/10.1002/2016WR019635) 597

Moon S, Huh Y, Qin J, Pho NV (2007) Chemical weathering in the 598
Hong (Red) River basin: rates of silicate weathering and their 599
controlling factors. *Geochim Cosmochim Acta* 600
71(6):1411–1430. <https://doi.org/10.1016/j.gca.2006.12.004> 601

Moore SJ, Anderholm SK (2002) Spatial and temporal variations in 602
streamflow, dissolved solids, nutrients, and suspended sediment 603
in the Rio Grande Valley study unit, Colorado, New Mexico, and 604
Texas, 1993–95. US Geological Survey, National Water-Quality 605
Assessment Program, Water-Resources Investigations Report 606
02-4224, Albuquerque, NM, 52 pp 607

Muigai PG, Shiundu PM, Mwaura FB, Kamau GN (2010) Correlation 608
between dissolved oxygen and total dissolved solids and their 609
role in the eutrophication of Nairobi dam, Kenya. *Int J of* 610
BioChemPhysics 18:38–46 611

Musolf A, Schmidt C, Selle B, Fleckenstein JH (2015) Catchment 612
controls on solute export. *Adv Water Resour* 86:133–146. 613
<https://doi.org/10.1016/j.advwatres.2015.09.026> 614

Nauditt A, Ribbe L (eds) (2017) Land use and climate change 615
interactions in central Vietnam. *Water Resources and* 616

- 617 Development, Springer Book Series. <https://doi.org/10.1007/978-981-10-2624-9>
- 618
- 619 Negrel P, Roy S, Petelet-Giraud E, Millot R, Brenot A (2007) Long-
- 620 term fluxes of dissolved and suspended matter in the Ebro River
- 621 Basin (Spain). *J Hydrol* 342(3–4):249–260. <https://doi.org/10.1016/j.jhydrol.2007.05.013>
- 622
- 623 Roy S, Gaillardet J, Allegre CJ (1999) Geochemistry of dissolved and
- 624 suspended loads of the Seine river, France: anthropogenic impact,
- 625 carbonate and silicate weathering. *Geochim Cosmochim Acta*
- 626 63(9):1277–1292. [https://doi.org/10.1016/S0016-7037\(99\)00099-X](https://doi.org/10.1016/S0016-7037(99)00099-X)
- 627 Sarin MM, Krishnaswami S, Dilli K, Somayajulu BLK, Moore WS
- 628 (1989) Major ion chemistry of the Ganga-Brahmaputra river
- 629 system: weathering processes and fluxes to the Bay of Bengal.
- 630 *Geochim Cosmochim Acta* 53(5):997–1009. [https://doi.org/10.1016/0016-7037\(89\)90205-6](https://doi.org/10.1016/0016-7037(89)90205-6)
- 631
- 632 Saunders JF, Lewis WM (1989) Transport of major solutes and the
- 633 relationship between solute concentrations and discharge in the
- 634 Apure River, Venezuela. *Biogeochemistry* 8(2):101–113. <https://doi.org/10.1007/BF00001315>
- 635
- Torres MA, West AJ, Clark KE (2015) Geomorphic regime modulates hydrologic control of chemical weathering in the Andes-Amazon. *Geochim Cosmochim Acta* 166:105–128. <https://doi.org/10.1016/j.gca.2015.06.007>
- White AF, Blum AE (1995) Effects of climate on chemical weathering in watersheds. *Geochim Cosmochim Acta* 59(9):1729–1747. [https://doi.org/10.1016/0016-7037\(95\)00078-E](https://doi.org/10.1016/0016-7037(95)00078-E)
- Xiao J, Jin Z-D, Ding H, Wang J, Zhang F (2012) Geochemistry and solute sources of surface waters of the Tarim River Basin in the extreme arid region, NW Tibetan Plateau. *J Asian Earth Sci* 54–55:162–173. <https://doi.org/10.1016/j.jseaes.2012.04.009>
- Zhang Q, Jin Z, Zhang F, Xiao J (2015) Seasonal variation in river water chemistry of the middle reaches of the Yellow River and its controlling factors. *J Geochem Explor* 156:101–113. <https://doi.org/10.1016/j.gexplo.2015.05.008>

UNCORRECTED PROOF